

Investigation of mechanism of metal ions adsorption from aqueous solutions using *Prosopis juliflora* roots: Batch and fixed bed column studies

Sujatha S.¹, Gokulan R.², Zunaithur Rahman³, and Yogeshwaran V.^{4*}

¹Department of Civil Engineering, K. Ramakrishnan College of Technology, Trichy, Tamil Nadu – 621112, India

²Department of Civil Engineering, GMR Institute of Technology, Srikakulam, Andhra Pradesh – 532 127, India

³Department of Civil Engineering, Aalim Muhammed Salegh College of Engineering, Avadi, Chennai – 600 055, India

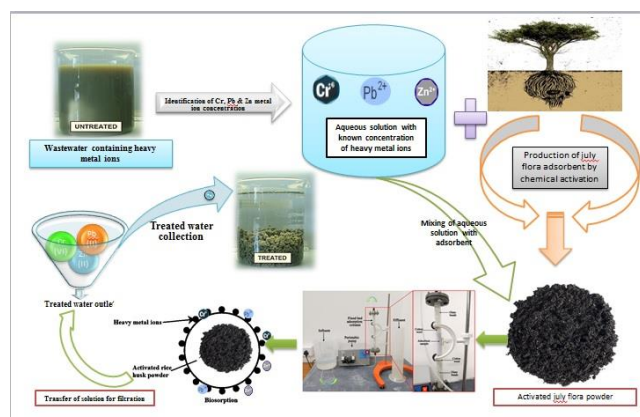
⁴Department of Civil Engineering, Sri Krishna College of Engineering and Technology, Coimbatore – 641008, India

Received: 02/10/2021, Accepted: 04/03/2022, Available online: 14/03/2022

*to whom all correspondence should be addressed: e-mail: svyogi23190@gmail.com

<https://doi.org/10.30955/gnj.004061>

Graphical abstract



Abstract

Adsorption of heavy metal ions (Cr, Pb & Zn) using *Prosopis Juliflora* roots has been investigated by batch adsorption and fixed bed column process. The various properties of adsorbent were analyzed and the FT-IR spectra & SEM studies of *Prosopis Juliflora* powder, before and after adsorption of metal ions also examined. From the batch adsorption study, maximum amount of metal ion adsorption was found to be 87.12% for Cr (VI), 92.28% for Pb (II) and 95.62% for Zn (II) metal ions. The Freundlich isotherm model fitted well than the Langmuir adsorption isotherm with high regression values. From the column study, optimum bed height of 5 cm, flow rate of 5 mL/min and metal ion concentration of 100 mg/L was obtained by breakthrough analysis. The fixed bed column study followed Thomas & Yoon-Nelson model plots with good correlations and maximum desorption rate was achieved by adding 0.3N of concentrated H₂SO₄.

Keywords: Adsorption, metal ions, isotherm studies, breakthrough analysis, kinetic modelling, desorption studies.

1. Introduction

Water pollution is one of the serious issues that we are facing from earlier stage. Clean water is required for all the communities, animals and plants, industrial process etc. Supply of clean water without any pollutants is one of the critical challenges and many countries are facing these kinds of problems from earlier stages (Akpen *et al.*, 2018). The water gets highly polluted in recent days due to extreme activities of industrial manufacturing and other pathogenic activities. Then the water becomes unsuitable for drinking due to changes in their physical and chemical properties (Badmus *et al.*, 2007). The pollution in water may be created by the presence of dyes, metal ions, suspended and dissolved solids and other organic & inorganic pollutants with very high concentration levels (Hasanpour *et al.*, 2020). Among various pollutants in the water, heavy metal pollution is one of the serious issues due to metal ion's toxicity and accumulation; it is very dangerous to the surrounding environment and human beings (Biswajit *et al.*, 2011). Increasing heavy metal pollution in day by day, the present world faces many health issues such as cancer, respiratory problems and other health issues (Table 1). Hence, it is necessary to reduce/remove the accumulation of heavy metal ions presents in the wastewater before discharging them into the water bodies. Many research works have been conducted to remove the accumulation of heavy metal ions from the wastewater (Yunnen *et al.*, 2017). To develop an innovative treatment process because of urgent need, the adsorption process has focused on removing metal ion concentration using batch and fixed bed process (Hasanpour *et al.*, 2021). This process has many advantages such as low capital cost, selective metal removal, desorption with no sludge generation (Qin *et al.*, 2015). Adsorption is the process of accumulation of atoms, ions or gaseous molecules to the adsorbate surface by batch mode or fixed bed column type (Hasfanila *et al.*, 2012). Using various adsorbate materials

(both natural and industrial waste), toxic metal ions has been removed by the adsorption process. Normally, the adsorbent material converted into activated carbon category for increasing the efficiency of adsorption process (Jiao *et al.*, 2012). Many natural adsorbents such as rice husk, neem leaves, saw dust, coconut shells rice bran etc., were used for removing different metal ion concentrations from the aqueous medium (Nadaffi *et al.*, 2007). Prosopis Juliflora Roots (PJR) is the type of organic material which is going to be used for removing the heavy metal ion contamination from aqueous solutions in this study. The Prosopis juliflora can penetrate their roots up to 60 m depth under the soli and consumes more amount of ground water (Lakshmipathy *et al.*, 2015). They are the type of small trees which is introduced in India during the year of 1877 to overcome the shortage of firewood. It has several environmental problems such as damage to landscapes, water storage areas, agricultural lands etc. (Li *et al.*, 2006). Indian government took several initiatives for removing the Prosopis juliflora trees from various places to protect level of ground water and surrounding environment. Figure 1(a) shows the distribution of Prosopis juliflora tress in the world, (b) shows the distribution pattern in India. There are too many

accumulations and distribution of trees are seen in the Figure 1 (a) & (b). Hence, it is decided to use the Prosopis juliflora roots as an adsorbent material to remove the heavy metal contamination in batch adsorption study.

2. Materials and methods

2.1. Preparation of adsorbent

The adsorbent sample (PJR) is collected in and around Ramanathapuram district, India. The collected samples are thoroughly washed with de-ionized water for removing the impurities and then dehydrated for 20 hrs at 200°C for eliminating solvent organic complexes. Using continuous grinding process, the adsorbent material was synthesized. Then the stock was cooled and washed several times for purification and dried to 80°C. Further, the samples are treated with concentrated HCl (0.3M) for removing the pathogenic bacteria and virus. The acid content in samples were removed by continuous washing by double distilled water and the samples are placed in an oven at 100°C about 24 hrs for removing the water content. Figure 2 shows the form of PJR, its physical properties has been analysed and mentioned in Table 2.

Table 1. Trace metals that may pose health hazards

S. No.	Element	Atomic No.	Sources	Health effects
1	Vanadium	23	Petroleum, Chemicals and catalysts, steel and other alloys	Probably no hazard at current levels
2	Chromium	24	Metal electroplating	A micronutrient to plant, chromates carcinogenic
3	Manganese	25	Mining and Industrial wastes	Relatively non-toxic, micro nutrient
4	Nickel	28	Fuel oil, coal, tobacco smoke, chemicals and catalysts, steel and non-ferrous alloys	Lung Cancer
5	Copper	29	Waste pipes, algae control, industrial smoke	Possible liver damage with prolonged exposure, toxic to plants
6	Zinc	30	Metal electro plating, mining, industrial smoke	Possible lung effects, low toxicity in solution
7	Arsenic	33	Coal, Petroleum, Detergents, Pesticides	Arsenic poisoning
8	Selenium	34	Coal, Sulphur	May cause dental caries, carcinogenic to rats, essential to mammals in low doses
9	Cadmium	48	Coal, Zinc mining, water mains and pipes, tobacco smoke	Cardiovascular disease and hypertension in human suspects interfere with zinc and copper metabolism
10	Lead	82	Auto Exhaust, Paints and water through lead joint of pipes	Brain damage, convulsions, behavioural disorder, fatality

Table 2. Physical Properties of chemically modified PJR powder

S.No	Physical Parameters	Range
1	Specific Gravity	0.53
2	Buk density (g/cc)	0.37
3	Porosity (%)	84
4	Surface area (m ² /g)	27
5	Avg. Particle size	10–47 µm
6	Moisture content (%)	39.2
7	Loss in ignition	93.22 (w/w %)
8	Al ₂ O ₃	2.2 (w/w %)

2.2. Preparation of metal ion solutions

100 mg of potassium di-chromate (K₂Cr₂O₇), lead sulphate (PbSO₄) and zinc chloride (ZnCl₂) has been mixed with 1 litre of double distilled water separately and the stock solutions were prepared. To obtain various design concentrations, the prepared water diluted with double distilled water. Using 0.1M of HCL, pH adjustments were carried out for entire studies.

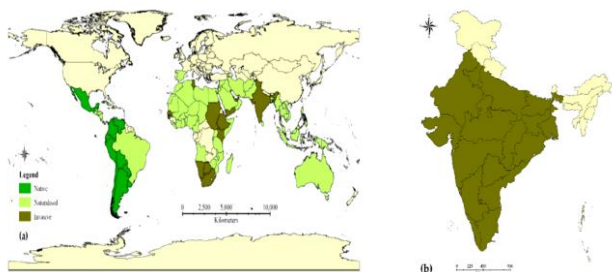


Figure 1. (a) Distribution of Prosopis juliflora in the world (b) Distribution status in India. Materials and methods.



Figure 2. Biochar derived from Prosopis juliflora roots.

2.3. Batch adsorption studies

Adsorption of heavy metal ions onto the adsorbent has been conducted through batch mode by adjusting the parameters of pH, contact time, adsorbent dose, metal ion concentrations and temperature. The impact of removal of heavy metal ions onto the adsorbent was examined with 50 mg/L of metal ion concentration 100 mL of solution with pH of 2.0 to 7.0 at 30°C, for the equilibrium period of 60 minutes. By varying the adsorbent dosage from 0.5 – 2.5 g/L the impact has been analysed. The conical flasks were kept on the rotary shaker, shaken for 60 minutes for ensuring attainment of equilibrium. The impact of contact time has been investigated by varying the time from 10 – 120 min. using the eqn. 1, the total amount of metal ions adsorbed onto the adsorbent has been calculated at various time intervals.

$$q_t = \frac{(C_o - C_t) V}{m} \text{ mg/g} \tag{2.1}$$

Where,

q_t – Amount of metal ion adsorbed onto the adsorbent at any time 't' (mg/g)

C_t – Concentration of batch adsorption processes

The metal ion solutions were centrifuged for 5 minutes and residual concentration of metal ions was found out using AAS. Each analysis was repeated twice and the results are taken from averages of these values. The percentage removal of the metal ions can be calculated by using the data obtained from batch studies. The mass balance relationship was obtained from the equation,

$$\% \text{ Removal} = \left[\frac{C_o - C_e}{C_o} \right] \times 100 \tag{2.2}$$

Where,

C_o – Initial concentration of the metal ion solution (mg/L)

C_e – Equilibrium concentration of the metal ion solution (mg/L)

V – Volume of the metal ion solution

m – Mass of the adsorbent used

For equilibrium studies, the initial concentration of metal ion solutions has been adjusted from 25 – 150 mg/L with 2 g/L of PJR dose at the pH of 6.0 in 100 mL solution. The temperature was fixed at 30°C and the solutions were shaken up to 60 minutes at a speed of 120 rpm in rotary shaker. Then the supernatant was taken for analysis using filter paper. The amount of metal ions adsorbed onto the adsorbent at equilibrium, q_e (mg/g) was calculated by,

$$q_e = \frac{(C_o - C_e) V}{m} \text{ mg/g} \tag{2.3}$$

Where,

C_o & C_e – Initial & equilibrium metal ion concentrations respectively (mg/l)

V – Volume of the metal ion solution

m – Mass of the adsorbent used

The impact on temperature has been investigated by Langmuir and Freundlich adsorption isotherm studies.

2.3.1 Langmuir isotherm model

It is based mainly on a few theories such as monolayer adsorption, adsorbate binding to the surface of the adsorbent happens predominantly by chemical reactions, and all sites have an equivalent preference for adsorbate (Putro *et al.*, 2017). This isotherm follows few assumptions such as, all the process are homogeneous, only one adsorbate used and this adsorbate molecules reacts with only one active site, in the adsorbate species no interactions are formed and the surface phase is monolayer (Musthapa *et al.*, 2019).

The Langmuir isotherm equation can be expressed in eqn. 2.4

$$\frac{C_e}{q_e} = \frac{1}{K \cdot q_{max}} + \frac{C_e}{q_{max}} \tag{2.4}$$

Where, C_e – Equilibrium concentration of the adsorbate solution

q_e – Amount of adsorbate adsorbed per gm.

K & q_{\max} – Langmuir constants related to the adsorption capacity and intensity.

2.3.2 Freundlich isotherm model

This isotherm model allows the multi-layer adsorption on the adsorbent surface (Akpomie *et al.*, 2015). The Freundlich isotherm equation can be expressed in eqn. 2.5.

$$\ln q_e = \ln k_f + \frac{1}{n} \ln C_e \quad (2.5)$$

Where, q_e – Amount of adsorbate adsorbed per gm

n – Energy of intensity or Adsorption

k_f – Freundlich constant related to adsorption capacity

C_e – Equilibrium concentration of the adsorbate solution

2.4 Column studies

To convert the batch adsorption study into pilot scale process, fixed bed column studies were performed under different conditions. A glass column with internal dia. of 2.5 cm & 30 cm length has been used to conduct the experimental analysis in the fixed bed adsorption process (Figure 3). By varying design parameters such as height of adsorbent bed (5 – 10 cm), concentrations of heavy metal ion solutions (100 – 300 mg/L) and flow rate of metal ion solutions (5 – 10 mL/min), the breakthrough analysis of the column has been examined. By Thomas and Yoon-Nelson kinetic plots, the equilibrium studies of adsorption process through fixed bed column have been investigated. The desorption studies of PJR adsorbent also carried out by concentrated H_2SO_4 (0.1 N, 0.2 N & 0.3 N) to identify the performance of fixed bed column. From the curve ' C_i/C_o vs t ', the breakthrough points were obtained and the performance of the fixed bed column study also evaluated.

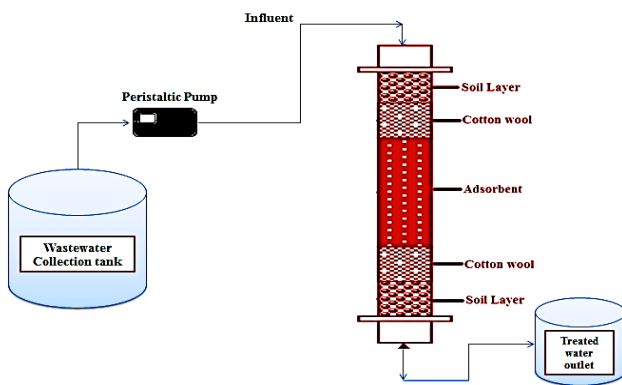


Figure 3. Experimental setup of fixed bed column

Using the equations from 2.6–2.10, the important parameters of the fixed bed column was calculated.

$$q_{total} = \frac{Q}{1000} \int_{t=0}^{t_{total}} C_{ad} dt \quad (2.6)$$

$$V_t = Qt_{total} \quad (2.7)$$

$$q_{bed} = \frac{q_{total}}{W} \quad (2.8)$$

$$M_{total} = \frac{C_o Qt_{total}}{1000} \quad (2.9)$$

$$\% removal = \frac{q_{total}}{M_{total}} * 100 \quad (2.10)$$

Where,

q_{total} – Total weight of metal ions adsorbed by the adsorbent in fixed bed column in mg

C_o – Initial metal ion concentration (mg/L)

C_{ad} – Initial and final metal ion concentration difference at the end of flow time in (mg/L)

V_t – Volume of treated effluent

Q – Volumetric flow rate (mL/min)

T_{total} – Total flow time

q_{bed} – Capacity of the bed (mg/g)

W – Weight of the adsorbent (g)

M_{total} – Total amount of metal ions added in the column

% removal – Total metal ions removal

2.4.1 Thomas model

To evaluate the performance of column and to examine prediction of breakthrough curves of a fixed bed column this Thomas model has been used extensively. The predominance of the plug flow dispersion is commonly occurring in the adsorption bed is the basic assumption of this model.

The Thomas model can be expressed in eqn. 2.11

$$\ln \left(\frac{C_o}{C_i} - 1 \right) = \frac{K_{th} q_o W}{Q} - K_{th} C_o t \quad (2.11)$$

By plotting $\ln \left(\frac{C_o}{C_i} - 1 \right)$ vs. time, the Thomas model parameters (K_{th} & q_o) were calculated.

Slope = $K_{th} C_o$

$$\text{Intercept} = \frac{K_{th} q_o W}{Q}$$

Where, C_i = Solute concentration (mg/L)

K_{th} = Thomas model constant (L/mg min)

q_o – Solid phase concentration of solute (mg/g)

w – Mass of the adsorbent (g)

Q – Volumetric flow rate (mL/min)

t – Time of flow (min)

2.4.2 Yoon-Nelson model

The Yoon-Nelson model applies primarily to a single system component and is straight forward without as many column variables. The model suggests that the rate of reduction in adsorption likelihood for growing adsorbate molecule is strongly related to the adsorbate breakthrough likelihood and adsorbate adsorption

possibility. The Yoon–Nelson Model can be expressed in eqn. 12.

$$\ln\left(\frac{C_i}{C_o - C_i}\right) = K_{YN}t - K_{YN}\tau \quad (2.12)$$

By plotting $\ln\left(\frac{C_i}{C_o - C_i}\right)$ vs. time gives the slope with

straight line of K_{YN} and the intercept of $-\tau K_{YN}$.

C_i – metal ion concentration of the effluent (mg/L)

C_o – initial metal ion concentration (mg/L)

K_{YN} – Yoon – Nelson constant (min^{-1})

τ – Time required for 50% of adsorbate breakthrough (min)

t – Time of flow (min)

To make the adsorption process more economical, it is necessary to regenerate the spent carbon (PJR) for further use. The desorption studies of fixed bed column were carried out by allowing the desorbing agents into the tired bed at suitable flow rates. At the exit point of the column bed, the solution (Cr, Pb and Zn) was collected at constant time intervals and its concentrations was analyzed. Then, all these samples (Cr, Pb and Zn) exposed to the adsorption studies once again until their enervation. In the desorption studies of fixed bed column, the desorbing solutions were not used from the batch adsorption study due to the structural damage of adsorbent at higher concentration levels and it reduces the ability of regeneration. Hence 0.3 N of H_2SO_4 solution is used to desorb chromium, lead and zinc ions respectively.

3. Results and discussion

3.1. Batch adsorption studies

3.1.1. FTIR

The FT – IR analysis of PJR and Cr (VI), Pb (II) & Zn (II) loaded PJR is shown in Figure 4. The spectrum of PJR and metal ions loaded PJR shows the amide –I group at 1650 cm^{-1} with strong band which indicates C=O stretching vibrations. At 1540 cm^{-1} , amide – II band has been raised in strong level which indicates the couplings of C –N stretching and N-H bending of C – N –H group. Amide – I & II are in constant position and strong intensities which are the characteristics of amides (M.A. Ahmad, 2014). At $3000 - 3400 \text{ cm}^{-1}$, the merged and broad band has been observed for –OH and –NH stretching. In case of metal ion loaded PJR, higher intensities become in very high peak and the maximum peak of amide band is shifted from 1650 to 1665 cm^{-1} , 1410 cm^{-1} shifted to 1415 cm^{-1} . Due to the presence of heavy metal ions in large amount in PJR this peak changes may be happened (Priya *et al.*, 2016). This shows that this PJR powder have higher adsorption capacity for metal ion removal.

3.1.2. SEM/EDX analysis

Referring Figures 5(a), (b), (c) and (d), the surface of adsorbent has been analysed before and after the adsorption of heavy metal ions. From Figure 5(a), the raw adsorbent (PJR) shows an irregular shape with lot of pores on their surface. From this, the surface morphology can

be identified in that adsorbent for adsorption of metal ions. The metal ions (Cr, Pb & Zn) loaded on the surface of PJR as shown if Figure 5(b), (c) & (d) respectively. From the figures, it was observed that the permeable site on the surface of PJR gets occupied by metal ions at the time of adsorption process (Sukumar *et al.*, 2017). The metal ions are adsorbed due to the presence of function groups in the inner walls of PJR surface. From the above discussion, it was observed that the PJR loaded with metal ions can be absorbed in the internal walls of adsorbent surface. The EDX image of raw and metal ion loaded adsorbent has been shown in Figure 5(a) & (b) and it confirms the presence of chromium, lead and zinc ions after the adsorption process. Apart from chromium, lead and zinc ions adsorbed, the raw adsorbent such as carbon, magnesium and sulphur are seen in EDX image of metal ion loaded adsorbent. Referring the Figure 5(a) & (b), additional metal elements/components were identified such as calcium, silica and sulphur. Due to acid treatment of tobacco leaves powder, the concentrated sulphuric acid reacts with hydroxyl groups presents in the adsorbent and forms sulphuric esters as a non-ionic functional group, which may complex cations (Yogeshwaran *et al.*, 2021). Hence it is concluded that the treatment with sulfuric acid solution protonates the charged sites and do not destroy any significant functional groups of raw adsorbent.

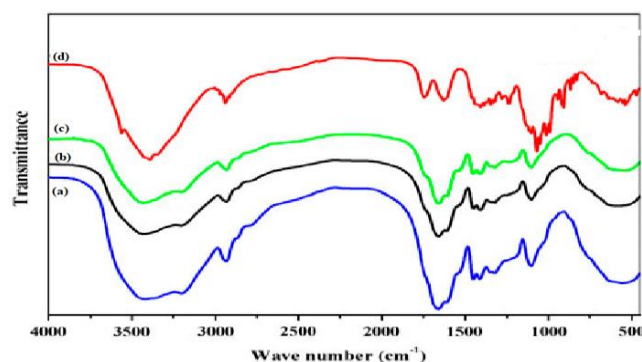


Figure 4. FT-IR Spectrum of (a) PJR, (b) Cr (VI), (c) Pb (II) and (d) Zn (II) adsorbed PJR.

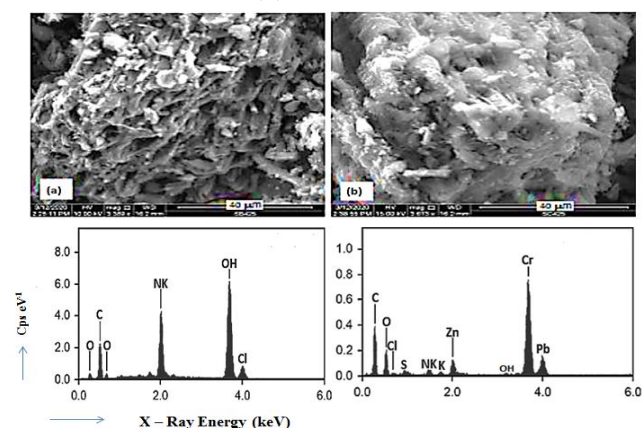


Figure 5. (a) & (b) SEM & EDX images of PJR before and after adsorption of metal ions

3.1.3. Impact of pH

Batch adsorption experiments were performed at different pH values (2.0 to 7.0). The amount of adsorption efficiency has been gradually increased (Figure 6) from 78.59 to 87.12% for Cr (VI), 88.63 to 92.28% for Pb (II) and

90.35 to 95.62% for Zn (II), with increase in the initial pH of the solution from 2.0 to 7.0. Figure 6 indicates that, at a lower pH level, the adsorbent surface was covered by hydronium ions (Ogunleye *et al.*, 2014). The adsorbent surface becomes more positively charged such that the interaction between adsorbent and metal ions is reduced (Zulfareen *et al.*, 2018). When the pH decreases, adsorbent surface becomes less positively charged and this promotes faster removal of metal ions. The adsorption of metal ions increases with an increase in solution's pH. The metal ions become less stable as there is an increase in solution's pH and adsorption reaches equilibrium at 6.0. However, at still higher pH values there is a decrease in removal of metal ions which is due to their precipitation of metal ions as their hydroxides (Vidhyadevi *et al.*, 2014). The influence of pH on adsorption could be explained by the presence of functional groups involved in metal ion uptake.

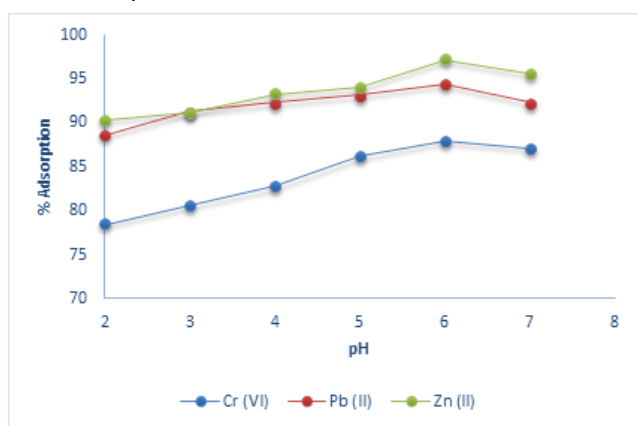


Figure 6. Impact of pH on Metal ion removal by PJR (Conc. = 50 mg/L, Dose = 1.5 g/L, Time = 90 min & Temp = 30°C).

3.1.4. Impact of adsorbent dosage

The impact of dosage level of the adsorbent onto the adsorption of metal ions such as Cr (VI), Pb (II) and Zn (II) was seen in Figure 7. In this plot, it was observed that the removal efficiency of metal ions onto the adsorbent were found to be 81.28% for Cr (VI), 71.82% for Pb (II) and 73.27% for Zn (II) at the dose of 2.5 g/L, and beyond this it remains almost constant. Due to the fall in the gradient concentration this may be happening in aqueous solution (Senthil kumar *et al.*, 2012). The rise in percentage of adsorption with an improvement in the adsorbent dosage could be attributed to an increase in the amount of free surfaces available, which has contributed to an increase in the number of adsorbent molecules (A.A. Alghamadi *et al.*, 2019). The optimum PJR dose was fixed as 2.5 g/L, and was applied to further experimental studies (Figure 8).

3.1.5. Impact of metal ion concentration

Initially adsorption experiments were carried out at low adsorbate concentration of 25 mg/L and the concentration level was gradually increased up to 150 mg/L with a common interval of 25 mg/L. From the plot 3.5, it was observed that the amount of adsorption efficiency was gradually decreased with the increase in metal ion concentration. Varying the metal ion concentrations from 25 – 150 mg/L for each metal ions (Cr, Pb and Zn) the percentage of adsorption decreased

from 90.8 to 60.4% for Chromium, 96.12 to 65.42% for Lead and 94.36 to 66.83% for zinc respectively. The amount of adsorption decreased evenly with the increase in metal ion concentration indicates that the adsorbent material did not reach the saturation (Agarwal *et al.*, 2006).

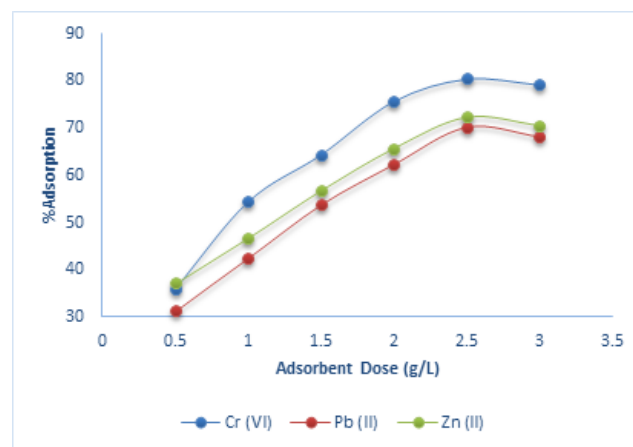


Figure 7. Impact of PJR dose on metal ion removal (Conc. = 50 mg/L, pH = 6.0, time = 90 min & Temp = 30°C).

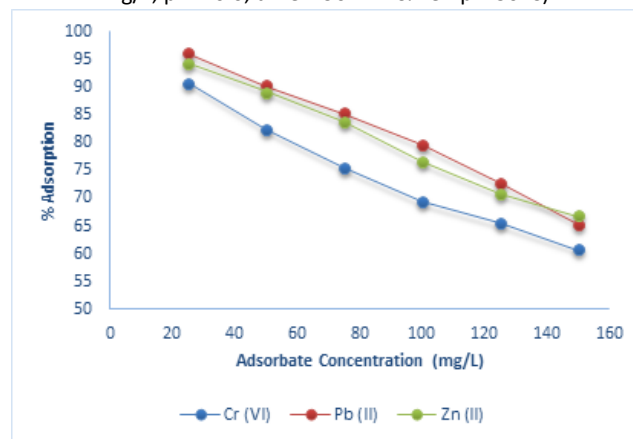


Figure 8. Impact of metal ion concentrations on Adsorption by PJR (Dose 2.5 g/L, pH = 6.0, time = 90 min & temp = 30°C).

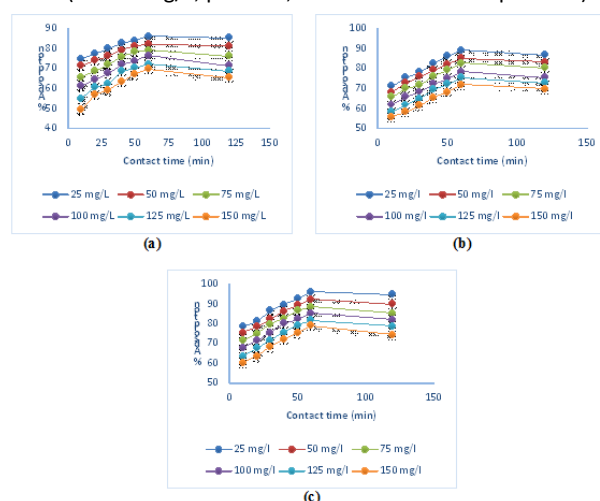


Figure 9. (a), (b) & (c) Impact of contact time on Cr, Pb & Zn metal ion adsorption (pH 6.0, Dose = 2.5 g/L, Temperature = 30°C & Conc. = 25 – 150 mg/L).

3.1.6. Impact of contact time

Varying the concentrations of metal ion solutions from 25 to 150 mg/L, impact of contact time between adsorbate

and metal ions has been investigated at the time interval from 10 to 120 min. The availability of vacant sites on the surface of adsorbent is higher and metal ion uptake was rapid during initial stages (Figure 9 (a), (b) & (c)). In addition, heavy metal ions are adsorbed onto the mesopores that get saturated (Dalia *et al.*, 2016). There was no significant changes were observed after 60 minutes of contact time and rate of adsorption reached constant value. This is because of repulsive forces in between the adsorbate molecules on solid surface (Ouyang *et al.*, 2019). Hence the mass transfer in between solid and liquid decreases with time of passage. Furthermore, metal ions are moved in deeper through pores with high strength which is slowing down of adsorption during the later phases (Amin *et al.*, 2017).

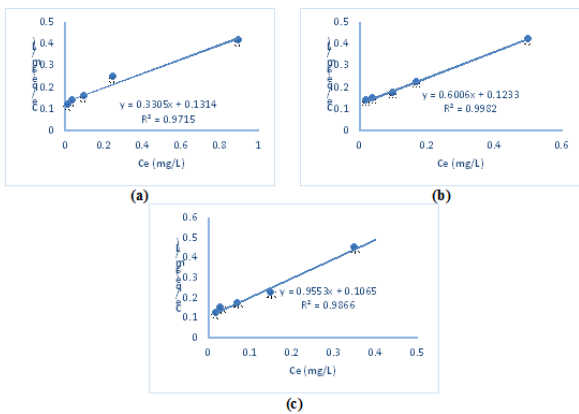


Figure 10. (a), (b) & (c) – Langmuir Isotherm plot for Cr, Pb & Zn ion adsorption using PJR.

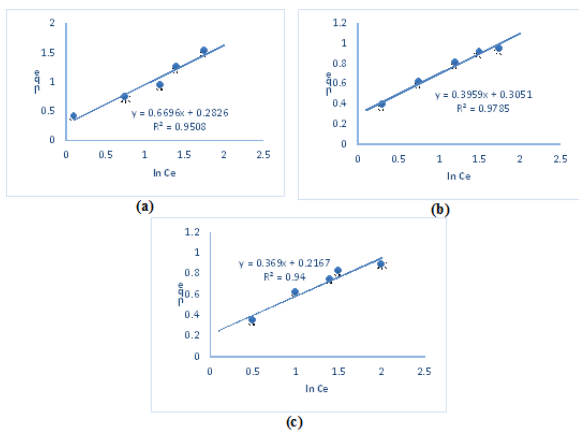


Figure 11. (a), (b) & (c) – Freundlich Isotherm plot for Cr, Pb & Zn ion adsorption using PJR.

Table 3 Isotherm constants for the removal of heavy metal ions by sugarcane bagasse

Isotherm Model	Metal ion solution			
	Parameters	Cr (VI)	Pb (II)	Zn (II)
Langmuir	q_{max} (mg/g)	8.304	8.992	9.344
	K_L (L/mg)	0.334	0.147	0.104
	R^2	0.9715	0.9982	0.9866
Freundlich	K_f ((mg/g) (L/mg) ^{1/n})	2.514	1.823	1.399
	n (g/L)	2.936	2.351	2.062
	R^2	0.9508	0.9785	0.9400

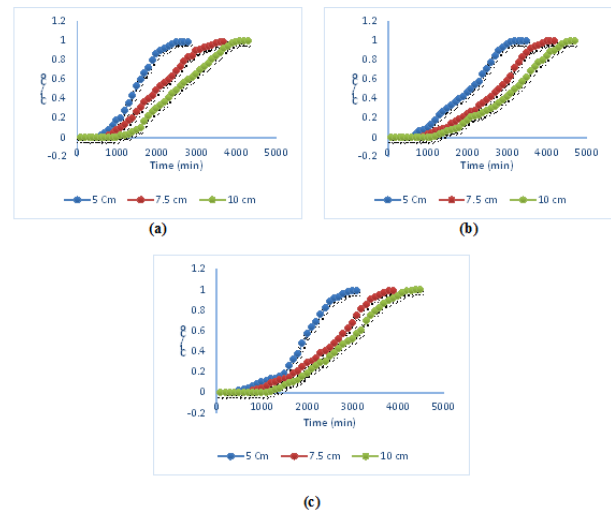


Figure 12. (a–c) Break through curve of Cr (VI), Pb (II), Zn (II) in different bed depths.

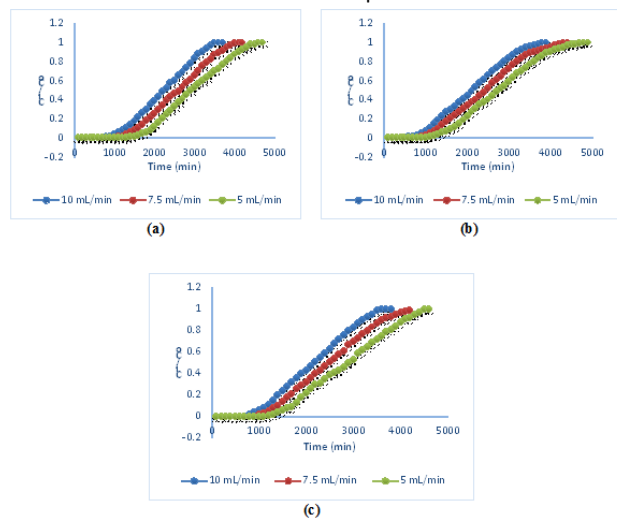


Figure 13. (a–c) Break through curve of Cr (VI), Pb (II), Zn (II) in different flow rate.

3.2. Adsorption isotherm studies

3.2.1. Langmuir isotherm

The Langmuir isotherm constants (k & q_{max}) and regression co-efficient values (R^2) were obtained by plotting the graph in between ' C_e/q_e ' vs. ' C_e '. Figure 10(a), (b) & (c) shows the linear plot of Cr (VI), Pb (II) & Zn (II) metal ions, and the values of Langmuir constants are calculated with the standard temperature of 30°C and represented in Table 3. From that table, it was observed that the k values are directly proportional to the q_{max} values and R^2 values are in $0.95 > R^2 < 1$ which indicates the adsorption process is favourable (Ali kara *et al.*, 2013).

Table 4. Breakthrough analysis parameters of adsorption of heavy metals at different bed heights

S.No	Type of Metal	Bed depth, Z (cm)	t_b (min)	V_t (mL)	T_{total} (min)	M_{total} (min)	q_{total} (mg)	q_{bed} (mg/g)	% Removal
1.	Cr (VI)	5	500	14000	2800	1400	1085.3	223.72	77.59
2.		7.5	700	18500	3700	1850	1526.2	289.26	82.57
3.		10	1000	21500	4300	2150	1887.7	347.63	87.84
4.	Pb (II)	5	600	17500	3500	1750	1034.2	203.36	59.18
5.		7.5	800	21000	4200	2100	1385.8	258.25	66.04
6.		10	1100	23500	4700	2350	1666.1	317.62	70.95
7.	Zn (II)	5	400	15500	3100	1550	1236.6	213.72	79.78
8.		7.5	700	19500	3900	1950	1661.4	279.35	85.24
9.		10	1100	22500	4500	2250	2000.2	335.43	88.97

Table 5. Breakthrough analysis parameters of adsorption of heavy metals at different flow rates

S.No	Type of Metal	Flow rate (Q) (mL/min)	t_b (min)	V_t (mL)	T_{total} (min)	M_{total} (min)	q_{total} (mg)	q_{bed} (mg/g)	% Removal
1.	Cr (VI)	5	1300	23500	4700	2350	1935.2	395.04	82.36
2.		7.5	1000	31500	4200	3150	2495.7	300.97	79.23
3.		10	700	37000	3700	3700	2875.6	225.3	77.72
4.	Pb (II)	5	1100	24500	4900	2450	1745.3	348.88	71.24
5.		7.5	800	33000	4400	3300	2271.7	302.72	68.84
6.		10	500	39000	3900	3900	2618.8	224.83	67.15
7.	Zn (II)	5	1100	23000	4600	2300	1884.3	376.46	80.19
8.		7.5	900	31500	4200	3150	2465.8	299.24	78.28
9.		10	700	38000	3800	3800	2932	214.89	77.16

3.2.2. Freundlich isotherm

The constants (K_f & n) of Freundlich isotherm model were calculated from the plot of $\ln q_e$ vs $\ln C_e$. Figure 11 (a), (b) & (c) shows the linear plots of Cr (VI), Pb (II) & Zn (II) metal ions, and the values of Freundlich constants are represented in Table 3. The constant of n values are > 1 was observed in that table, which indicates the metal ion adsorption follows physical adsorption process. Similarly, the values of R^2 are in $0.95 > R^2 < 1$ which indicates the adsorption process is favourable. By referring R^2 values in Table 3, the metal ion adsorption using PJR was fitted well in Freundlich isotherm model, than Langmuir isotherm model. This is recognized on the metal ion adsorption by PJR in monolayer (Koohzad *et al.*, 2019). From the above discussions, it was concluded that the metal ion adsorption onto the adsorbent follows heterogeneous and monolayer adsorption mechanism (Boudrahen *et al.*, 2011).

3.3. Fixed bed column study

3.3.1. Breakthrough analysis

Varying the bed height from 5 – 10 cm by fixing metal ion concentration of 100 mg/L and flow rate of 5 mL/min, the impact has been analysed in the column. Referring Figure 12(a), (b), (c) S – shaped curve was obtained for Cr (VI), Pb (II), Zn (II) metal ion removal. With increase in bed height from 5 – 10 cm, the breakthrough time and time of exhaust also increased. From the plots, the breakthrough time has been attained at 10 cm adsorptive bed height. Staying time of heavy metal ions in adsorbent bed increases better adsorption and longer contact time (Ashraf Ali *et al.*, 2016). Also, there is a possibility to have additional active binding sites for the adsorption of heavy

metal ions (Gopal *et al.*, 2016). The metal ion concentration has been fixed at 100 mg/L and adsorptive bed height at 10 cm, impact of fixed bed adsorption was investigated by varying rate of flow from 5 – 10 mL/min. In general, the rate of flow is inversely proportional to adsorbed metal ions. Based on this suggestion, it was identified that the breakthrough time has attained at 5 mL/min of flow rate (Figure 13(a), (b) & (c)), for Cr (VI), Pb (II) & Zn (II) metal ion removal. The turbulence of flow has been increased during the maximum rate of flow and further decreases the mass transfer resistance from external sources marked at the particle surfaces of the adsorbent (H.A. Hezagi, 2013). This is the reason for earlier breakthrough and the rate of metal ions adsorption on to surface of adsorbent has to be increased leading to quick saturation (H. Patel, 2019). From 100 to 300 mg/L of heavy metal ion concentrations (Cr, Pb & Zn) the impact has been investigated by fixing the flow rate of 5 mL/min and bed height of 10 cm. Referring Figure 14 (a), (b) & (c), at the earlier stages, breakthrough time has not arrived in low metal ion concentrations due to large number of effluents. The gradient has been developed in lower concentrations and decreases the diffusion coefficient. Also, the adsorbent has established slower transport of metal ions on their surfaces. During initial stages, at higher metal ion concentrations the adsorbent bed gets saturated quickly with metal ions and leads to fast breakthrough (Karunarathne *et al.*, 2013). Also, the mass transfer increased by driving forces at higher metal ion concentrations (Kalaivani *et al.*, 2015). Hence, the amount of adsorption decreases with decrease in metal ion concentrations. Tables 4–6 indicates the adsorption rate of Cr (VI), Pb (II) & Zn (II) metal ions using breakthrough analysis.

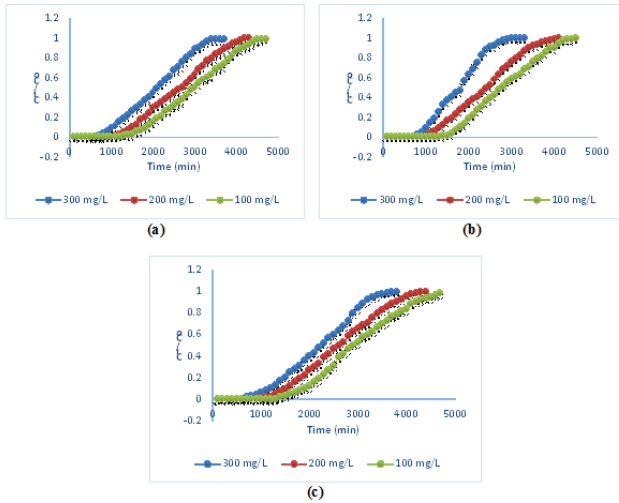


Figure 14. (a–c) Break through curve of Cr (VI), Pb (II), Zn (II) in different metal ion concentrations.

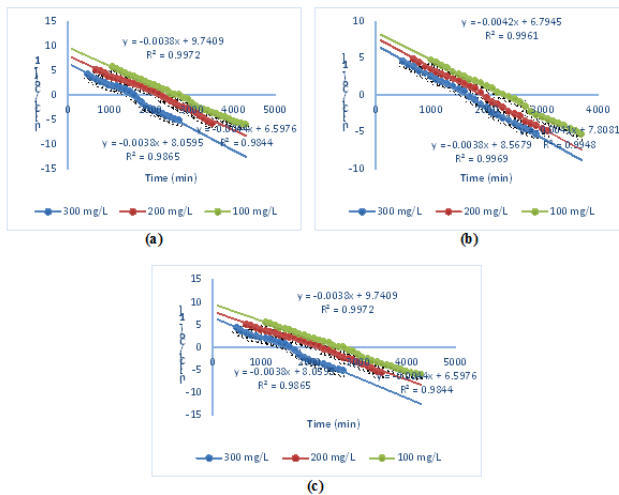


Figure 15. (a–c) Thomas model plots in different Cr (VI), Pb (II) and Zn (II) ion Concentrations.

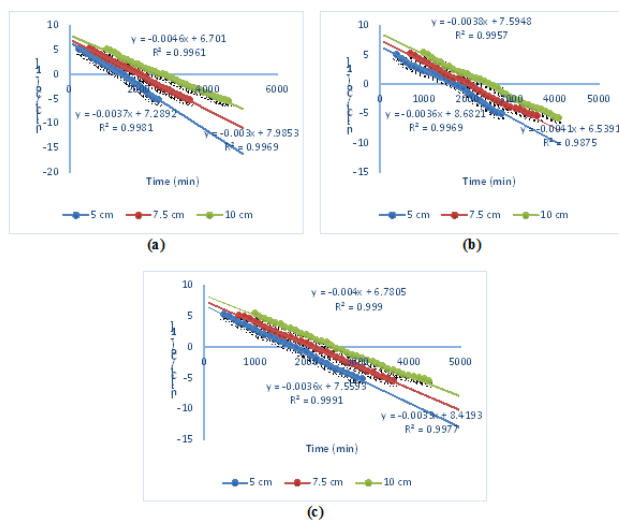


Figure 16. (a–c) Thomas model plots in different bed depths of Cr (VI), Pb (II) and Zn (II) ions.

3.3.2. Kinetic studies

(a) Thomas model

The adsorption capacity of fixed bed column and Thomas model constant (q_0 & K_{th}) were analysed by adjusting the rate of flow from 5 – 10 mL/min, concentrations of metal ions from 100 – 300 mg/L and adsorbent bed height from 5 – 10 cm. By varying the conditions in this experimental work, Thomas model has shown very high regression values ($R^2 > 0.95$). The rate of flow and Thomas model constant has been increased with decrease in adsorption capacity was identified by referring the Tables 7–9. On the other hand, the Thomas model constant (K_{th}) values were decreased with increase in metal ion concentrations. This is because of higher metal ion concentrations levels the driving force is very high and this has happened due to the very high difference in metal ion concentrations at the phases of adsorbate and adsorbent (Lalitha *et al.*, 2018). This process leads to increase in capacity of adsorption during the higher metal ion concentrations. Similar trend has been developed by changing the height of adsorbent bed. Hence, for better achievement of adsorption rate and performance of the column, lower flow rate, higher metal ion concentrations and optimum bed height is needed (Mahmud *et al.*, 2016). From Figure 15 (a), (b) and (c) for Cr (VI), 16 (a), (b) and (c) for Pb (II) and 17 (a), (b) and (c) for Zn (II) the parameters of the Thomas model were calculated.

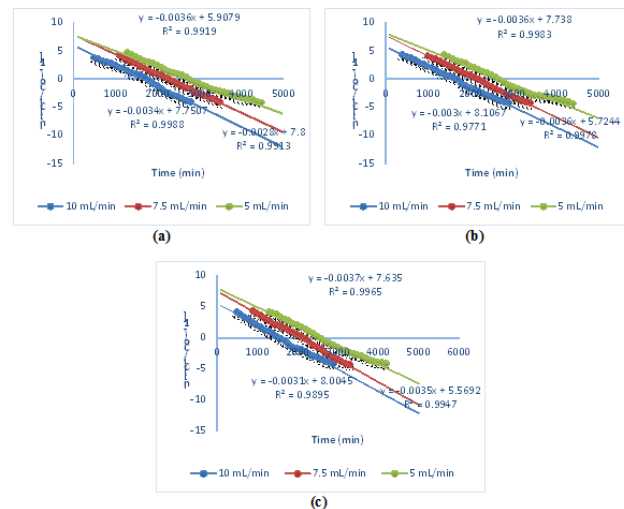


Figure 17. (a–c) Thomas model plots in different flow rates of Cr (VI), Pb (II) and Zn (II) solutions.

(b) Yoon-Nelson model

Adjusting the flow rate from 5 – 10 mL/min, adsorbate bed height from 5 to 10 cm and concentrations of metal ions from 100 – 300 mg/L, Yoon-Nelson model was investigated. The two basic parameters of Yoon – Nelson model (rate constant - K_{YN} & time required - τ) were obtained from the plot of $\ln [C_i / (C_0 - C_i)]$ vs. time (t) (Figures 18–20) and the values are mentioned in Tables 10–12 for Cr (VI), Pb (II) & Zn (II) metal ion adsorption respectively. From the plots of Yoon-Nelson model, it was identified that an attainment of straight line along with slope and intercept. Referring Tables 10–12, the values of ' K_{YN} ' and ' τ ' are inversely proportional. For 50%

breakthrough time (τ) increases, the rate constant values were gradually decreased by the variations of rate of flow, metal ion concentrations and height of bed (Jain *et al.*, 2013). This is attributable to the fact that too many metal ions compete for adsorption sites at higher concentrations of metal ions due to higher adsorption sites leads to rapid uptake of metal ions (Sathish *et al.*, 2015).

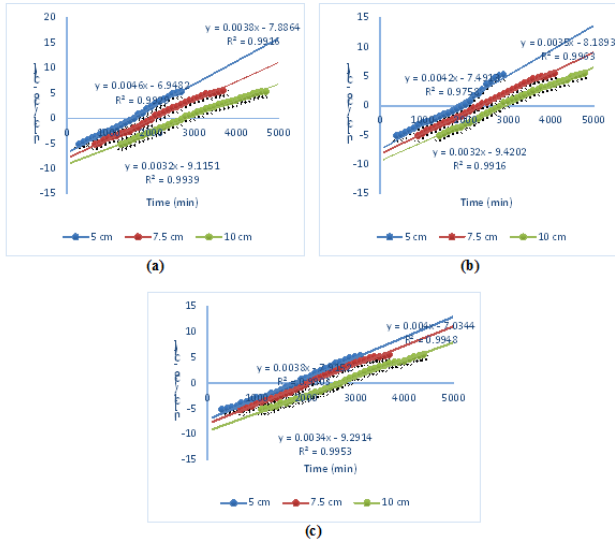


Figure 18. (a), (b), (c) – Yoon - Nelson plots in different bed depths of Cr (VI), Pb (II) and Zn (II) ions.

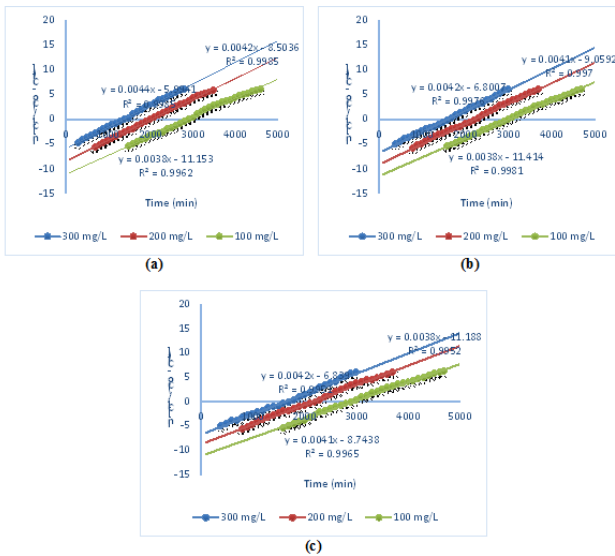


Figure 19. (a-c) – Yoon - Nelson plots in different Cr (VI), Pb (II) and Zn (II) ion Concentrations.

3.4. Desorption and regeneration

Varying the molarity of concentrated H₂SO₄ (0.1 – 0.3N), desorption studies has been carried out in continuous mode with rate of flow of 5 mL/min and the desorbing solution is allowed into exhaustion bed. The concentration of solution was investigated in every 5 minutes time interval at the exit of column setup. The elution curve of chromium solution in fixed bed column is shown in Figure 21(a). By referring the curves, up to optimum point the rate of desorption has been increased gradually and after that it starts decreasing for all three eluents of 0.1, 0.2 &

0.3N (Renu *et al.*, 2020). Similar trend also followed for lead and zinc solutions. The maximum amount of desorption rate of 870 mg/L was observed at 0.3 N of H₂SO₄ for chromium ions in 30 minutes. Also, 780 mg/L of desorption rate was observed at 50 minutes for lead ions (Figure 21(b)) and 850 mg/L of desorption rate was observed at 40 minutes for zinc ions (Figure 21(c)) with 0.3N of H₂SO₄. The performance of fixed bed column has been identified by reuse of adsorbent. Hence, desorption process has been conducted up to their saturation level by three different cycles. Regeneration and further usage of set up decided the performance of the column (Bayuo *et al.*, 2020). The efficiency of regeneration (η) can be calculated by ratio of capacity (Q_{reg}) of adsorption after the regeneration and unique adsorption capacity (Q_{org}) of the column (eqn. 3.1). Figure 22 shows the regeneration cycles of adsorption processes for chromium, lead and zinc ions with 0.3 M of H₂SO₄.

$$\eta = \frac{Q_{org} - Q_{reg}}{Q_{org}} \quad (13)$$

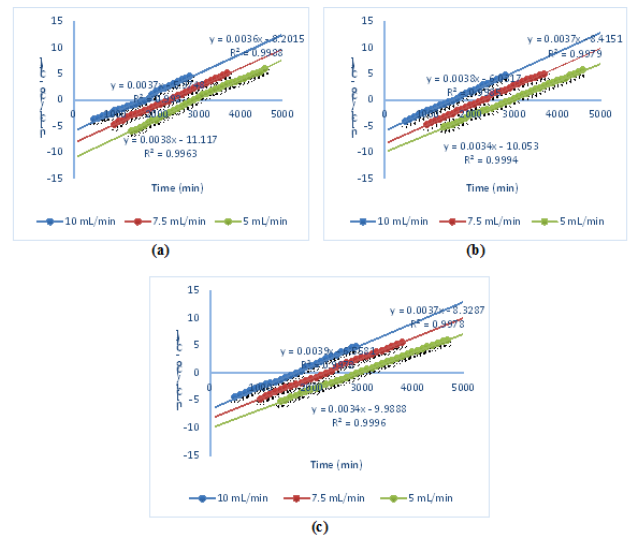


Figure 20. (a-c) Yoon - Nelson plots in different flow rates of Cr (VI), Pb (II) and Zn (II) metal ions.

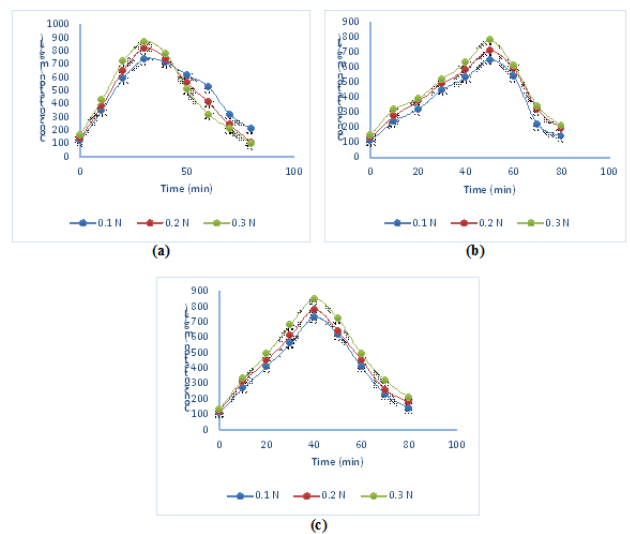


Figure 21. (a-c) Desorption rate plots of Cr (VI), Pb (II) & Zn (II) using H₂SO₄.

Table 6. Breakthrough analysis parameters of adsorption of heavy metals at different metal ion concentrations

S.No	Type of Metal	Ion Conc. (C ₀) (mg/L)	t _b (min)	V _t (mL)	T _{total} (min)	M _{total} (min)	q _{total} (mg)	q _{bed} (mg/g)	% Removal
1.	Cr (VI)	100	1100	23500	4700	2350	1900.1	365.4	80.85
2.		200	900	21500	4300	4300	3280.9	436.8	76.32
3.		300	500	18500	3700	5550	3966.5	495.3	71.47
4.	Pb (II)	100	1200	23000	4600	2300	1670.2	340.8	72.62
5.		200	900	21500	4300	4300	2985.4	439.6	69.43
6.		300	600	16500	3300	4950	3309	378.1	66.85
7.	Zn (II)	100	1300	24000	4800	2400	1950	410.5	81.25
8.		200	900	22000	4400	4400	3468.9	462.5	78.84
9.		300	600	19000	3800	5700	4415.7	496.1	76.53

Table 7. Thomas model – Calculated parameters for chromium ion adsorption

S.No.	Slope	Intercept	C ₀ (mg/L)	K _{th} (min ⁻¹ mg ⁻¹ L)	Z (cm)	Q (mL/min)	q ₀
1.	-0.0046	6.47	300	1.54 x 10 ⁻⁵	5	5	387.45
2.	-0.00364	7.67	200	1.82 x 10 ⁻⁵	5	5	342.83
3.	-0.00369	10.63	100	3.69 x 10 ⁻⁵	5	5	251.28
4.	-0.00457	6.70	100	4.57 x 10 ⁻⁵	5	5	238.26
5.	-0.00366	7.28	100	3.66 x 10 ⁻⁵	7.5	5	264.83
6.	-0.00298	7.98	100	2.98 x 10 ⁻⁵	10	5	287.32
7.	-0.00360	5.90	100	3.60 x 10 ⁻⁵	5	5	253.24
8.	-0.00344	7.75	100	3.44 x 10 ⁻⁵	5	7.5	225.47
9.	-0.00280	7.80	100	2.80 x 10 ⁻⁵	5	10	198.26

Table 8. Thomas model – Calculated parameters for lead ion adsorption

S.No.	Slope	Intercept	C ₀ (mg/L)	K _{th} (min ⁻¹ mg ⁻¹ L)	Z (cm)	Q (mL/min)	q ₀
1.	-0.0044	6.59	300	1.46 x 10 ⁻⁵	5	5	381.26
2.	-0.0037	8.05	200	1.85 x 10 ⁻⁵	5	5	352.35
3.	-0.0037	9.74	100	3.70 x 10 ⁻⁵	5	5	264.37
4.	-0.0040	6.53	100	4.0 x 10 ⁻⁵	5	5	243.45
5.	-0.0037	7.59	100	3.70 x 10 ⁻⁵	7.5	5	267.36
6.	-0.0035	8.68	100	3.50 x 10 ⁻⁵	10	5	289.34
7.	-0.0035	5.72	100	3.50 x 10 ⁻⁵	5	5	261.24
8.	-0.0036	7.73	100	3.60 x 10 ⁻⁵	5	7.5	239.32
9.	-0.0030	8.10	100	3.0 x 10 ⁻⁵	5	10	202.31

Table 9. Thomas model – Calculated parameters for zinc ion adsorption

S.No.	Slope	Intercept	C ₀ (mg/L)	K _{th} (min ⁻¹ mg ⁻¹ L)	Z (cm)	Q (mL/min)	q ₀
1.	-0.0042	6.79	300	1.40 x 10 ⁻⁵	5	5	380.54
2.	-0.0041	7.80	200	2.05 x 10 ⁻⁵	5	5	327.43
3.	-0.0037	8.56	100	3.70 x 10 ⁻⁵	5	5	264.24
4.	-0.0039	6.78	100	3.90 x 10 ⁻⁵	5	5	232.54
5.	-0.0035	7.55	100	3.50 x 10 ⁻⁵	7.5	5	258.43
6.	-0.0032	8.41	100	3.20 x 10 ⁻⁵	10	5	272.74
7.	-0.0035	5.56	100	3.50 x 10 ⁻⁵	5	5	256.46
8.	-0.0036	7.63	100	3.60 x 10 ⁻⁵	5	7.5	235.24
9.	-0.0030	8.00	100	3.0 x 10 ⁻⁵	5	10	204.56

Table 10. Yoon - Nelson model – Calculated parameters for chromium ion adsorption

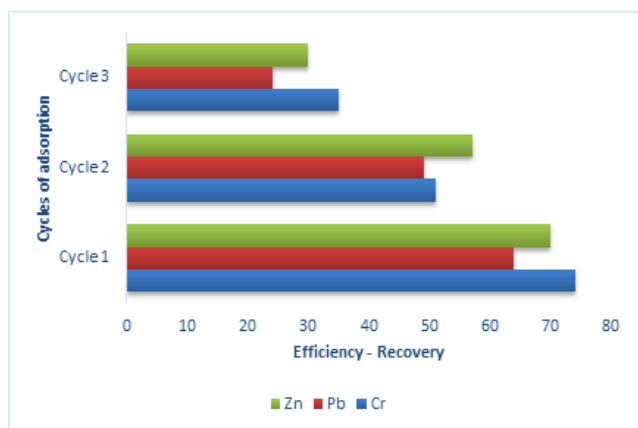
S.No.	Intercept	C ₀ (mg/L)	K _{VN} (min ⁻¹)	Z (cm)	Q (mL/min)	τ (min)
1.	5.99	300	0.0044	5	5	1429
2.	8.50	200	0.0042	5	5	2075
3.	11.15	100	0.0038	5	5	2938
4.	6.94	100	0.0045	5	5	1638
5.	7.88	100	0.0037	7.5	5	2047
6.	9.11	100	0.0031	10	5	2756
7.	5.97	100	0.0037	5	5	1765
8.	8.20	100	0.0036	5	7.5	2384
9.	11.11	100	0.0038	5	10	2965

Table 11. Yoon - Nelson model – Calculated parameters for lead ion adsorption

S.No.	Intercept	C ₀ (mg/L)	K _{VN} (min ⁻¹)	Z (cm)	Q (mL/min)	τ (min)
1.	6.87	300	0.0042	5	5	1655
2.	9.05	200	0.0041	5	5	2239
3.	11.41	100	0.0038	5	5	3046
4.	7.49	100	0.0042	5	5	1938
5.	8.18	100	0.0035	7.5	5	2374
6.	9.42	100	0.0032	10	5	2856
7.	6.03	100	0.0038	5	5	1667
8.	8.41	100	0.0037	5	7.5	2353
9.	10.05	100	0.0034	5	10	2978

Table 12. Yoon - Nelson model – Calculated parameters for zinc ion adsorption

S.No.	Intercept	C ₀ (mg/L)	K _{VN} (min ⁻¹)	Z (cm)	Q (mL/min)	τ (min)
1.	6.83	300	0.0042	5	5	1763
2.	8.74	200	0.0038	5	5	2256
3.	11.18	100	0.0041	5	5	2948
4.	7.03	100	0.0040	5	5	1864
5.	7.91	100	0.0038	7.5	5	2436
6.	9.29	100	0.0034	10	5	2743
7.	6.55	100	0.0039	5	5	1759
8.	8.32	100	0.0037	5	7.5	2362
9.	9.98	100	0.0034	5	10	2984

**Figure 22.** Regeneration of fixed bed column.

4. Conclusion

The performance of biosorption of heavy metal ions (Cr, Pb & Zn) was investigated using PJR in batch and fixed bed adsorption process. The maximum adsorption efficiency was obtained at the pH of 6.0, contact time of 1 hr, metal ion concentration of 100 mg/L, adsorbent dosage of 2.5 g/L with the constant temperature of 30°C. Both Langmuir and Freundlich isotherm models were fitted well in this batch adsorption process with high correlations. In the fixed bed column, volume of treated effluent has been analysed by breakthrough curves at various time intervals. Thomas and Yoon-nelson models are fitted well with best correlation values in fixed bed adsorption process. The maximum desorption rate of metal ions (Cr, Pb & Zn) was observed with the addition of 0.3 N of concentrated H₂SO₄. Furthermore, the maximum recovery of metal ions was obtained in the first cycle with concentrated H₂SO₄ acid. From the experimental results, PJR powder has

shown its excellent adsorptive capacity of heavy metal ions from the aqueous solutions.

References

- Agarwal G.S., Bhuptawat H.K. and Chaudhari.S. (2006). Biosorption of aqueous chromium (VI) by tamarindus indica seeds. *Bioresource Technology*, **97**, 949–956.
- Ahmad M.A. (2014). Kinetic, equilibrium and thermodynamic studies of synthetic dye removal using pomegranate peel activated carbon prepared by microwave – induced KOH activation. *Water Resources and Industry*, **06**, 18–35.
- Akpen G.D., Aho M.I. and Baba N. (2018). Adsorption of cadmium (II) from simulated wastewater using albizia samanpod activated carbon in fixed bed columns. *Nigerian Journal of Technology*, **37**, 833–840.
- Akpomie K.G., Dawodu F.A. and Adebowale K.O. (2015). Mechanism on the sorption of heavy metals from binary-solution by a low-cost montmorillonite and its desorption potential. *Alexandria Engineering Journal*, **54**, 757–767.
- Alghamdi A.A., Odayni A.B.A., Saeed W.S., Kahtani A.L., Alharthi F.A., and Aouak T. (2019). Efficient Adsorption of Lead (II) from aqueous phase solutions using polypyrrole – based activated carbon. *Materials*, **12**.
- Ali A., Saeed K., and Mabood F. (2016). Removal of Chromium (VI) from aqueous medium using chemically modified banana peels as efficient low-cost adsorbent. *Alexandria Engineering Journal*, **55**, 2933–2942.
- Amin M.T., Alazba A.A. and Shafiq M. (2017). Batch and fixed bed column studies for the biosorption of Cu (II) and Pb (II) by raw and treated date palm leaves and orange peel. *Global Nest Journal*, **19**, 464–478.
- Badmus M.A.O., Audu T.O.K., and Anyata B.U. (2007). Removal of Lead Ion from Industrial Wastewaters by Activated Carbon Prepared from Periwinkle Shells (*Typanotonus fuscatus*).

- Turkish Journal of Engineering and Environmental Sciences*, **31**, 251–263.
- Bayuo J., Abukari M.A. and Pelig – Ba K.B. (2020). Desorption of chromium (VI) and lead (II) ions and regeneration of the exhausted adsorbent. *Applied Water Science*, **9**, 171.
- Boudrahem F., Aissani – Benissad F. and Soualah A. (2011). Adsorption of Lead (II) from aqueous solution by using leaves of date trees as an adsorbent. *Journal of Chemical & Engineering Data*, **56**, 1804–1812.
- Christian Taty-Costodes V., Fauduet H., Porte C., and Yuh-Shah Ho. (2005). Removal of lead (II) ions from synthetic and real effluents using immobilized pinus sylvestris saw dust: Adsorption on a fixed bed column. *Journal of Hazardous Materials*, **B123**, 135–144.
- Dalia I. Sanchez-machado., Jaime lopez-cervantes., Ma.A. Murrieta. and Reyna G. Sanchez-Duarte. (2016). Modelling breakthrough curves for aqueous iron (III) adsorption on chitosan –sodium tripolyphosphate. *Water Science and Technology*, **74**, 2297–2304.
- Gopal N., Asaithambi M., Sivakumar P. and Sivakumar V. (2016). Continuous fixed bed adsorption studies of rhodamine – B dye using polymer bound adsorbent. *Indian Journal of Chemical Technology*, **23**, 53–58.
- Hasanpour M. and Hatami M. (2020). Application of three-dimensional porous aerogels as adsorbent for removal of heavy metal ions from water/wastewater: A review study. *Advances in Colloid and Interface Science*, **284**, 102247.
- Hasanpour M., Motahari S., Jing D., and Hatami M. (2021). Investigation of operation parameters on the removal efficiency of methyl orange pollutant by cellulose/zinc oxide hybrid aerogel. *Chemosphere*, **284**, 131320.
- Hasfalina C.M., Maryam C.A., Luqman R.Z. and Rashid M. (2012). Adsorption of Copper (II) from aqueous medium in fixed bed column by kenaf fibres. *APCBEE Procedia*, **3**, 255 – 263.
- Hegazi H.A. (2013). Removal of heavy metals from wastewater using agricultural and industrial wastes as adsorbents. *HRBC Journal*, **9**, 276–282.
- Jain M., Kumar Garg V. and Kadirvelu K. (2013). Removal of Ni (II) from aqueous system by chemically modified sunflower biomass. *Desalination and Water Treatment*, **52**, 5681–5695.
- Jiao C., Cheng Y., Fan W. and Li J. (2012). Synthesis of agar – stabilized nanoscale zero valent iron particles and removal study of hexavalent chromium. *International Journal of Environmental Science Technology*, **12**, 1603–1612.
- Kalaivani S.S., Vidhyadevi T., Murugesan A., Thiruvengadaravi K.V., Anuradha D. and Sivanesan S. (2015). The use of new modified poly (acrylamide) chelating resin with pendent benzothiazole groups containing donor atoms in the removal of heavy metal ions from aqueous solutions. *Water Resources India*, **5**, 21–35.
- Kalavathy Karthikeyan M.H., Rajgopal T. and Miranda L.R. (2007). Kinetic and isotherm studies of Cu (II) adsorption onto HPO-activated rubber wood sawdust. *Journal of Colloidal Interface Sciences*, **292**, 354–362.
- Kara A., Ustun G.E., Solmaz S.K.A., and Demirbel E. (2013). Removal of Pb (II) ions in fixed bed column from electroplating wastewater of bursa, an industrial city in turkey. *Journal of Chemistry*, **ID: 953968**.
- Karunarathe H.D.S.S. and Amarasinghe B.M.W.P.K. (2013). Fixed bed adsorption column studies for the removal of aqueous phenol from activated carbon prepared from sugarcane bagasse. *Energy Procedia*, **34**, 83–90.
- Koohzad E., Jafari D., and Esmaeili H. (2019). Adsorption of lead and arsenic ions from aqueous solution by activated carbon prepared from Tamarix Leaves. *Chemistry Europe*, **04**.
- Lakshmipathy R. and Sarada N.C. (2015). A fixed bed column study for the removal of Pb²⁺ ions by watermelon rind. *Environmental science: Water Research & Technology*, **1**, 244–250.
- Lalitha L.M. and Mariraj Mohan S. (2018). Performance evaluation of multibed adsorbent on removal of hexavalent chromium through various kinetic models. *Journal of Environmental Engineering and Landscape Management*, **26**, 285–298.
- Li Q., Zhai W., Zhang W., Wang M. and Zhou J. (2006). Kinetic studies of adsorption of Pb (II), Cr (III) and Cu (II) from aqueous solution by sawdust and modified peanut husk. *Journal of Hazardous Materials*, **141**, 163–167.
- Mahmud., H.N.M.E. Huq. and A.O. binti Yahya. (2016). The removal of heavy metal ions from wastewater/aqueous solution using polypyrrole-based adsorbents - A review. *RSC Advances*, **06**, 14778–14791.
- Musthapa S., Shuaib D.T., Ndamisto M.M., Etsuyankpa M.B., Sumaila A., Mohammad U.M. and Nasirudeen M.B. (2019). Adsorption isotherm, kinetic and thermodynamic studies for the removal of Pb (II), Cd (II), Zn (II) and Cu (II) ions from aqueous solutions using Albizia lebeck pods. *Applied Water Science*, **9**, 142.
- Naddafi K., Nabizadeh R., Saeedi R., Mahvi A.H., Vaezi F., Yaghmaeian K., Ghasri A. and Nazmara S. (2007). Biosorption of lead (II) and Cadmium (II) by protonated sargassum glaucescens biomass in a continuous packed bed column. *Journal of Hazardous Materials*, **147**, 785–791.
- Ogunleye O.O., Ajala M.A., and Agarry S.E. (2014). Evaluation of biosorptive capacity of banana (*Musa paradisiaca*) stalk for lead (II) removal from aqueous solution. *Journal of Environmental Protection*, **05**, 1451-1465.
- Ouyang D., Zhuo Y., Hu L., Zeng Q., Hu Y., and He Z. (2019). Research on the adsorption behaviour of heavy metal ions by porous material prepared with silicate tailings. *Minerals*, **9**, 291.
- Patel H. (2019). Fixed bed column adsorption study: a comprehensive review. *Applied Water Science*, **9**, 45.
- Priya A.K., Nagan S., Nithya M., Priyanka P.M. and Rajeswari M. (2016). Assessment of tendu leaf refuses for the heavy metal removal from electroplating effluent. *Journal of Pure and Applied Microbiology*, **10**, 585-591.
- Putro J.N., Santoso S.P., Ismajli S. and Ju Y.H.. (2017). Investigation of heavy metal adsorption in binary system by nanocrystalline cellulose – Bentonite nanocomposite: Improvement on extended Langmuir isotherm model. *Microporous and Mesoporous Materials*, **246**, 166–177.
- Qin F., Wen B., Shan X.Q., and Xie Y.N. (2015). Mechanisms of competitive adsorption of Pb, Cu and Cd on peat. *Environmental Pollution*, **144**, 669–680.
- Renu., Agarwal M., Singh K., Gupta R., and Dohare R.K. (2020). Continuous fixed bed adsorption of heavy metals using biodegradable adsorbent: Modelling and experimental study. *Journal of Environmental Engineering*, **146**, 04019110.
- Sangha B., Naiya T.K., Bhattacharya A.K., and Das S. (2011). Cr (VI) ions removal from aqueous solutions using natural

- adsorbents – FTIR studies. *Journal of Environmental Protection*, **2**, 729–735.
- Sathish T., Vinithkumar N.V., Dharani G., and Kirubakaran R. (2015). Efficacy of mangrove leaf powder for bioremediation of chromium (VI) from aqueous solutions: kinetic and thermodynamic Evaluation. *Applied Water Sciences*, **5**, 153–160.
- Senthil Kumar P., Ramalingam S., Sathyaselvabala V., Dinesh Kirupha S., Murugesan A., and Sivanesan S. (2012). Removal of cadmium (II) from aqueous solution by agricultural waste cashew nut shell. *Korean Journal of Chemical Engineering*, **29**, 756–768.
- Sukumar C., Janaki C., Vijayaraghavan K., Kamala Kannan S. and Shanthi K. (2017). Removal of Cr (VI) using co-immobilized activated carbon and *Bacillus subtilis*: fixed bed column study. *Clean Technologies and Environmental Policy*, **19**, 251–258.
- Vidhyadevi T., Murugesan A., Kalaivani S.S., Premkumar M.P., Vinothkumar V., and Ravikumar L. (2014). Evaluation of equilibrium, kinetic, and thermodynamic parameters for adsorption of Cd²⁺ ion and methyl red dye onto amorphous poly(azomethinethioamide) resin. *Desalination and Water Treatment*, **52**, 3477–3488.
- Yogeshwaran V. and Priya A.K. (2021). Adsorption of lead ion concentration from the aqueous solution using tobacco leaves. *Materials Today: Proceedings*, **37**, 489–496.
- Yunnen C., Ye W., Chen L., Lin G., Jinxian N., and Rushan R. (2017). Continuous fixed bed column study and adsorption modelling: Removal of arsenate and arsenic in aqueous solution by organic modified spent grains. *Polish Journal of Environmental Studies*, **26**, 1847–1854.
- Zulfareen N., Venugopal T., and Sajitha I. (2018). Removal of zinc from synthetic wastewater by activated carbon *Prosopis juliflora*. *International Journal of Advanced Science and Engineering*, **4**, 746–749.